Heat Transfer Capacity of Lotus-Type Porous Copper Heat Sink*

Hiroshi CHIBA**, Tetsuro OGUSHI**, Hideo NAKAJIMA*** and Teruyuki IKEDA***

Lotus-type porous copper is a form of copper that includes many straight pores, which are produced by the precipitation of supersaturated gas dissolved in the molten metal during solidification. The lotus-type porous copper is attractive as a heat sink because a higher heat transfer capacity is obtained as the pore diameter decreases. We investigate a fin model for predicting the heat transfer capacity of the lotus-type porous copper. Its heat transfer capacity is verified to be predictable via the straight fin model, in which heat conduction in the porous metal and the heat transfer to the fluid in the pores are taken into consideration by comparison with a numerical analysis. We both experimentally and analytically determine the heat transfer capacities of three types of heat sink: with conventional groove fins, with groove fins that have a smaller fin gap (micro-channels) and with lotus-type porous copper fins. The conventional groove fins have a fin gap of 3 mm and a fin thickness of 1 mm, the micro-channels have a fin gap of 0.5 mm and a fin thickness of 0.5 mm, and the lotus-type porous copper fins have pores with a diameter of 0.3 mm and a porosity of 0.39. The lotus-type porous copper fins were found to have a heat transfer capacity 4 times greater than the conventional groove fins and 1.3 times greater than the micro-channel heat sink under the same pumping power.

Key Words: Porous Media, Lotus-Type Porous Copper, Fin Efficiency, Heat Transfer Capacity, Heat Sink

1. Introduction

In recent years, heat dissipation rates in power devices and high frequency electronic devices have been increasing, and as a result, heat sinks with high heat transfer performance are required to cool these devices. Heat sinks utilizing micro-channels with channel diameters of several tens of microns are expected to have excellent cooling performance because a higher heat transfer capacity is obtained with smaller channel diameters.

Heat transfer performance of micro-channel constructed in silicon wafers has also been studied(1). To enhance the cooling performance of heat sinks with micro-channels, Wei and Joshi(2) investigated three-dimensional stacked micro-channel heat sinks. Porous materials are considered preferable for three-dimensional micro channels, highlighted by Bastawros'(3) study on cellular metal as a heat transfer medium. Among porous materials such as sintered porous metal, cellular metal and fibrous composite, lotus-type porous metal with straight pores is preferable for heat sinks due to the small pressure drop of cooling water flowing through the pores.

In this work, we investigate the use of lotus-type porous copper in micro-channel heat sinks. An outer view of the lotus-type porous copper is shown in Fig. 1. The lotus-type porous copper is made of copper with many straight pores that are formed by precipitation of supersaturated gas dissolved in the melted copper during solidification. Such lotus-type porous metals can be fabricated by the Czochralski, casting and zone melting methods(4). The main features of lotus-type porous metals are as follows;

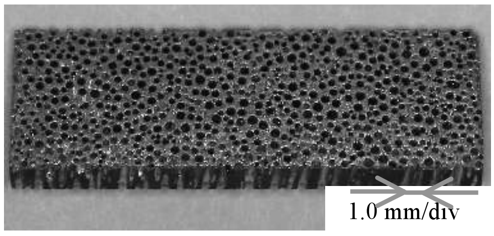

Fig. 1 Outer view of lotus-type porous copper

* Received 2nd February, 2004 (No. 04-4045)
** Mechanical Systems Department, Adv. Tch., R&D Cent., Mitsubishi Electric Corporation, 8–1–1 Tsukaguchi Honmachi, Amagasaki, Hyogo 661–8661, Japan. E-mail: Chiba.Hiroshi@wrc.melco.co.jp
*** The Institute of Scientific and Industrial Research, Osaka University, Ibaraki, Osaka 567–0047, Japan

(1) the pores are straight, (2) the pore size and porosity are controllable, and (3) the porous metals with pores whose diameter is as small as ten microns can be produced.

For the design of heat sinks using the lotus-type porous copper, it is necessary to introduce the fin model of the lotus copper. So, it is crucial to know the effective thermal conductivity of the lotus copper, considering the pore effect on heat flow. Behrens[5] investigated the effective thermal conductivities of composite materials analytically and proposed a simple equation for predicting the effective thermal conductivity. Han and Conser[6] have conducted a numerical investigation into the effective thermal conductivities of fibrous composites.

In the previous work, we applied Behrens' analytical equation to the effective thermal conductivity of the lotus copper perpendicular to the pore axis and compared with these results the experimental data, in which the porosity changed. The experimental data on the thermal conductivity of lotus copper perpendicular to the pore axis $k_{\mathrm{eff}\perp}$ showed good agreement with the Behrens equation[7].

In the present work, we investigate a straight fin model for predicting the heat transfer capacity of lotus copper. This model takes into consideration the heat conduction in the porous metal and the heat transfer to the fluid in the pores. We compare results produced with the model with the numerical analysis in a case where the spacing between pores and the heat transfer coefficient in the pores are changed.

Furthermore we examine the heat transfer capacity of three types of heat sinks: one with conventional groove fins, one with a smaller groove fins (micro-channels), and one using lotus-type porous copper. The conventional groove fin has a fin gap of 3 mm and a fin thickness of 1 mm, which the micro-channels have a fin gap of 0.5 mm and a fin thickness of 0.5 mm. The lotus-type porous copper fins have pores with an average diameter of 0.3 mm and a porosity of 0.39.

2. Nomenclature

A_b : base plate area of heat sink [m^2]
A_c : cross-sectional area of fin [m^2]
De : hydraulic diameter [m]
dp : average diameter of pores [m]
f_g : fin gap [m]
h : heat transfer coefficient [W/(m$^2\cdot$K)]
H_f : fin height [m]
h_i : heat transfer coefficient based on A_b [W/(m$^2\cdot$K)]
$k_{\mathrm{eff}\perp}$: effective thermal conductivity perpendicular to pore axis [W/(m$\cdot$K)]
k_l : liquid thermal conductivity [W/(m$\cdot$K)]
k_s : material thermal conductivity [W/(m$\cdot$K)]
L : length of groove fin along flow direction [m]
Nu_g : Nusselt number defined by fin gap
Nu_p : Nusselt number defined by average diameter of pores
P_f : peripheral length of straight fin [m]
Pr : Prandtl number
ΔP : pressure drop of heat sink [Pa]
Q : heat flow [W]
q : heat flux [W/m^2]
Re_d : Reynolds number defined by hydraulic diameter
Re_g : Reynolds number defined by fin gap
Re_p : Reynolds number defined by average diameter of pores
S_f : total surface area of pores [m^2]
T_b : temperature of copper base plate [K]
T_i : inlet temperature of cooling water [K]
T_o : outlet temperature of cooling water [K]
T_s : surrounding temperature [K]
ΔT : temperature difference [K]
U : flow rate [m^3/s]
u : velocity [m/s]
Δx : heat flow distance [m]

Greek symbol
ε : porosity
η : fin efficiency

3. Analysis of Fin Efficiency

3.1 Straight fin model

In order to predict the heat transfer capacity of the lotus copper, it is necessary to consider the heat conduction in the porous metal and the heat transfer to the fluid in the pores. The heat transfer capacity of the heat conducting body to transfer heat to the surroundings from its surface is generally expressed by a fin model. By contrast, in the lotus-type porous copper heat sink, heat is input from the top surface and flows downward by heat conduction, with the heat transferred to the fluid in the pores along the way as shown in Fig. 2 (a). The lotus copper fin, is modeled as

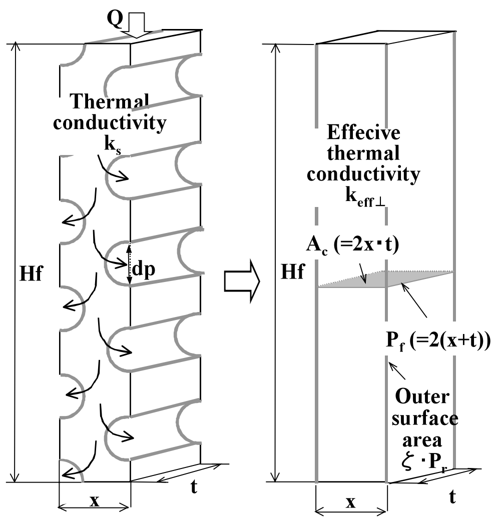

(a) Lotus copper fin (b) Straight fin model

Fig. 2 Analytical lotus fin model

straight fin as shown in Fig. 2 (b). The heat transfer rate Q under temperature difference ΔT between the top surface of the fin and the fluid in the pores is calculated from Eq. (1),

$$Q = h \cdot S_f \cdot \eta \cdot \Delta T \quad (1)$$

where η is fin efficiency, S_f is the total surface area of the pores and h is the heat transfer coefficient in the pores.

In the straight fin, the fin efficiency is expressed as the following:

$$\eta = \frac{\tanh(m \cdot H_f)}{m \cdot H_f} \quad (2)$$

$$m = \sqrt{\frac{h \cdot \zeta \cdot P_f}{k_{\mathrm{eff}\perp} \cdot A_c}} \quad (3)$$

where H_f is the fin height, $k_{\mathrm{eff}\perp}$ is the effective thermal conductivity perpendicular to the pore axis and P_f is the peripheral length of the fin. Furthermore A_c is the cross-sectional area of the fin, while ζ is the ratio between the total surface area of the lotus copper S_f and the total surface area of the straight fin $P_f \cdot H_f$, which can be expressed as the following,

$$\zeta = \frac{S_f}{P_f \cdot H_f} \quad (4)$$

3.2 Numerical analysis

In order to verify the efficiency of the straight fin model, we conducted a numerical analysis to predict the fin effectiveness, The numerical model of the lotus copper is shown in Fig. 3.

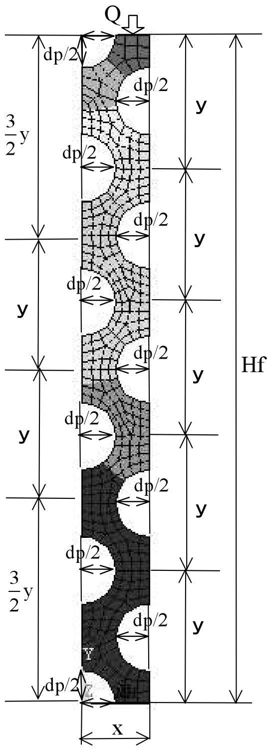

Fig. 3 Numerical model to predict fin efficiency

The mean temperature ΔT between the top surface of the fin model and the surrounding temperature T_s in the pores were calculated using the finite differential method under the following boundary conditions; uniform heat input Q at the top surface, uniform heat transfer coefficient h in the pores, and a constant surrounding temperature T_s.

In the calculation, the spacing of pores (x,y) and h were changed under the conditions of pore diameter dp of 200 μm and a material thermal conductivity k_s of 400 W/(m·K).

A comparison of the fin efficiency η between the numerical results and results from Eq. (2) is shown in Fig. 4. Equation (2) showed good agreement with the numerical simulation; therefore the fin efficiency of the lotus fin η was verified to be predictable by Eq. (2) derived from the straight fin model.

3.3 Investigated heat sinks

We examine the heat transfer capacity of the three types of heat sink- with conventional groove fins, groove fins with smaller fin gaps (micro-channel) and lotus-type porous copper. The configuration and the specifications of the conventional groove fins and micro-channels are shown in Fig. 5 and Table 1. The conventional groove fins have a fin gap of 3 mm and a fin thickness of 1 mm. The micro-channels have a fin gap of 0.5 mm and a fin thickness also of 0.5 mm. The heat transfer capacity of the con-

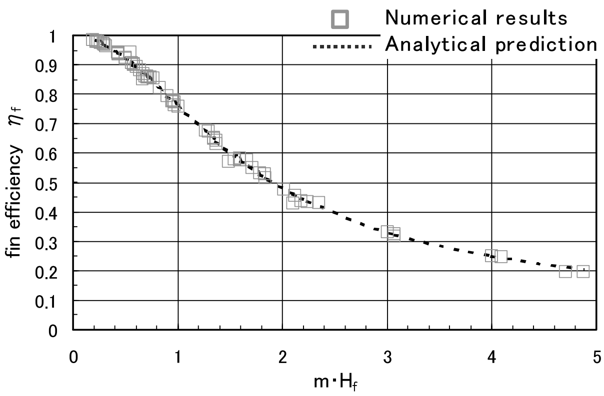

Fig. 4 Comparison of fin efficiency between numerical results and analytical prediction from Eq. (2)

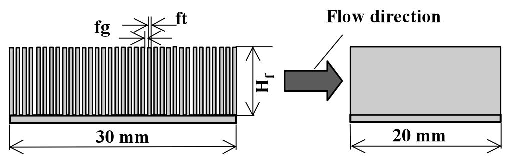

Fig. 5 Conventional groove fins and micro-channels

Table 1 Specifications of conventional groove fins and micro-channels

	Fin gap fg (mm)	Fin tichkness ft (mm)	Fin Height Hf (mm)	Investigation
Conventional groove fins	3	1	9	Calc.
Micro-channels	0.5	0.5	9	Calc. & measured

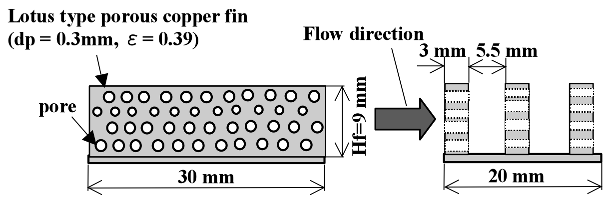

Fig. 6 Lotus-type porous copper heat sink

ventional groove fins is a calculated one only.

Figure 6 shows the configuration of the lotus-type porous copper heat sink, which features three lotus copper fins with lengths of 3 mm along the flow direction. The lotus-type porous copper fins have pores with a mean diameter of 0.3 mm and a porosity of 0.39.

3.4 Heat-transfer capacity and pressure drop of heat sinks experimental method

Figure 7 shows the experimental apparatus for measuring the heat transfer capacity of heat sink. Cooling water was circulated through a filter and the test duct in which the heat sink is located. The circulator has a pump and water cooling equipment. The heat sink itself consists of fins that are brazed on one side of a copper base plate. The heating block with a heater is soldered onto the other side of the base plate. Inlet temperature of the cooling water T_i, the temperature of the copper base plate T_b, and the outlet temperature of the cooling water T_o are measured by K type thermocouples.

We evaluated the heat transfer capacity by heat transfer h_i based on the base plate area A_b as follows,

$$h_i = \frac{Q}{A_b \cdot (T_b - T_i)} \tag{5}$$

where Q is the heat transfer rate evaluated by deducting the heat loss through the thermal insulator around the heater from heat input. The pressure drop between the inlet and the outlet of the fins of all the heat sinks were measured within an experimental accuracy of ±5% by a pressure sensor (Krone Corp., model: DP-15).

3.5 Predictions of the heat transfer coefficient and pressure drop

3.5.1 Conventional groove fins and micro-channels

Correlations for the heat transfer coefficient and a pressure drop of the conventional groove fins and micro-channels are expressed by the following equations under the laminar flow regime ($Re < 3\,000$)[8],[9],

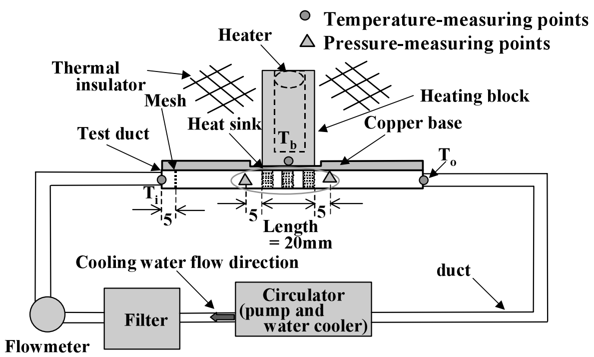

Fig. 7 Experimental apparatus for measuring the heat transfer capacity

$$Nu_g = \frac{Nu_1 - Nu_2}{10 - 0.71} \cdot (Pr - 0.71) + Nu_2 \tag{6}$$

$$Nu_1 = 2.801\,36 - 2.105\,14X^* + 0.411\,783X^{*2} + 4.11 \tag{7}$$

$$Nu_2 = 4.188\,80 - 3.147\,09X^* + 0.611\,075X^{*2} + 4.11 \tag{8}$$

$$X^* = \ln\left(\frac{L}{f_g} \cdot Re_g \cdot Pr\right), \tag{9}$$

where Re_g is the Reynolds number defined by the fin gap $(= u \cdot f_g/\nu)$, Nu_g is the Nusselt number defined by the fin gap $(= h \cdot f_g/k_l)$, L is the length of the groove fin along the flow direction, u is the velocity of a fluid through the fin gaps, ν is the dynamic viscosity of the fluid, and k_l is the thermal conductivity of the fluid.

$$f = \frac{3.44}{X^{0.5} \cdot Re_d} + \frac{24 + \left(\frac{0.674}{4 \cdot X}\right) - \left(\frac{3.44}{X^{0.5}}\right)}{(1 + 0.000\,029 \cdot X^{-2}) \cdot Re_d} \tag{10}$$

$$X = L/(Re_d \cdot De) \tag{11}$$

$$\Delta P = f \cdot \left(\frac{4L}{De}\right) \cdot \left(\frac{1}{2}\rho u^2\right) \tag{12}$$

Here De is the hydraulic diameter $(= 4f_g \cdot H_f / 2(f_g + H_f))$, and Re_d is Reynolds number $(= u \cdot De/\nu)$.

3.5.2 Lotus-type porous copper fins

As the flow characteristics through the pores in the lotus copper fins are considered to be similar in a cylindrical pipe, the heat transfer coefficient and pressure drop of the lotus copper fins are expressed by the following correlations for the circle pipe under laminar flow regime ($Re < 3\,000$)[10]:

$$Nu_p = 5.364\left(1 + \{(220/\pi)X^+\}^{-10/9}\right)^{3/10} \times \left\{1 + \left(\frac{\pi/(115.2X^+)}{[1 + (Pr/0.020\,7)^{2/3}]^{1/2}\left[1 + \{(220/\pi)X^+\}^{-10/9}\right]^{3/5}}\right)^{5/3}\right\}^{3/10} - 1 \tag{13}$$

$$X^+ = (L/dp)/(Re_p \cdot Pr) \tag{14}$$

$$\Delta P = \left(\frac{64}{Re_p}\right) \cdot \left(\frac{L}{dp}\right) \cdot \left(\frac{1}{2}\rho u^2\right), \tag{15}$$

where Re_p is the Reynolds number ($= u \cdot dp/\nu$), and Nu_p is Nusselt number ($= h \cdot dp/k_l$).

3.6 Experimental data

3.6.1 Heat transfer capacity The heat transfer coefficients based on base-plate surface area A_b defined by Eq. (5) for the experiment of results and Eq. (16) for the calculated results are plotted for all of heat sinks as a function of the inlet velocity to the heat sinks u_o in Fig. 8.

$$h_i = \frac{h \cdot S_f \cdot \eta}{A_b} \tag{16}$$

The prediction for the lotus-type porous copper heat sink showed good agreement with the experimental data within an accuracy of ±15%. The experimental data for the lotus-type porous copper heat sink showed a very large heat transfer coefficient of 80 000 W/(m^2·K) under the velocity u_o of 0.2 m/s, which is 1.7 times higher than that for the micro-channels and 6.5 times higher than that for the conventional groove fins.

3.6.2 Pressure drop The pressure drops in all of the heat sinks are compared in Fig. 9 as a function of u_o. The predicted pressure drop of the lotus-type porous copper heat sink showed good agreement with the experimental data within an accuracy of ±5%.

On comparing the pressure drop among all of the heat sinks at a velocity u_o of 0.2 m/s, experimental results show that the pressure drop of the lotus-type porous copper heat sink is 2.5 times greater than that of the micro-channels and 38 times greater than that of the conventional groove fins.

4. Discussion

Figure 10 shows the heat transfer coefficient h_i as a function of ΔP. On comparing the heat transfer coefficients among all of the heat sinks under the same pressure drop, the experimental data for the lotus-type copper heat sink is around 1.2 times greater than that of the micro-channels and twice as greater as that of the conventional

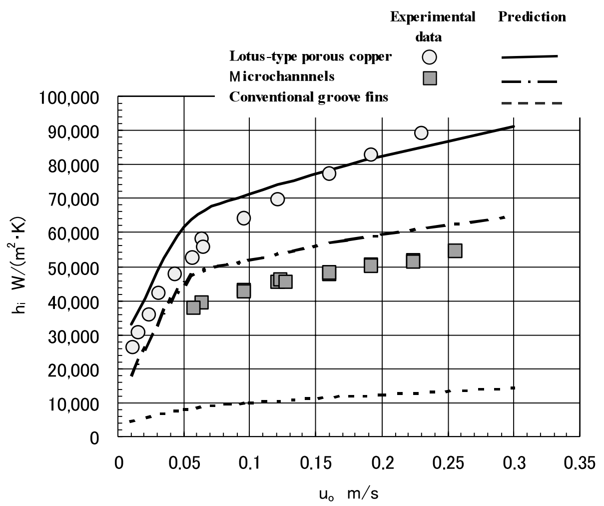

Fig. 8 Comparison of heat transfer h_i between experimental and predicted data

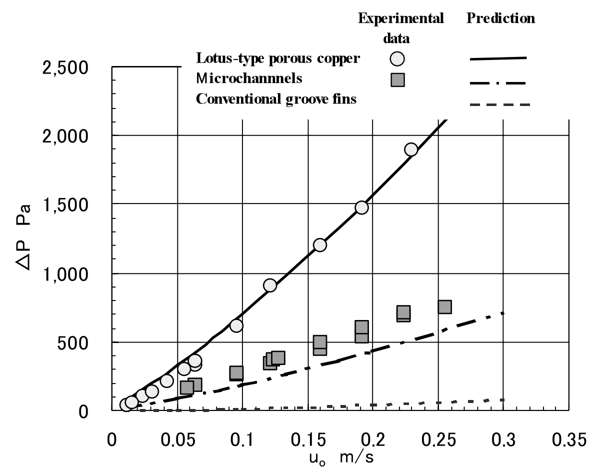

Fig. 9 Comparison of pressure drop ΔP between experimental and predicted data

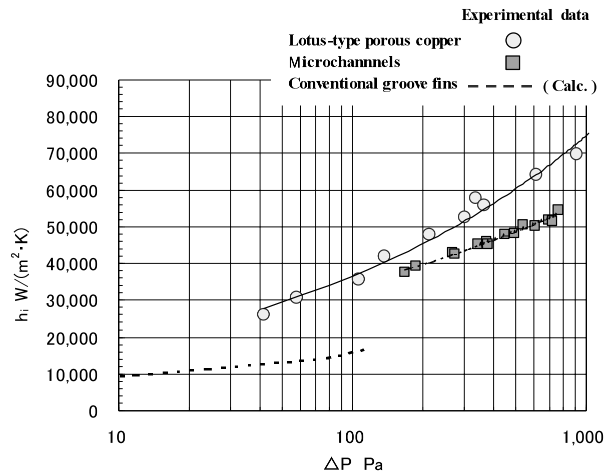

Fig. 10 Comparison of heat transfer h_i as a function of pressure drop

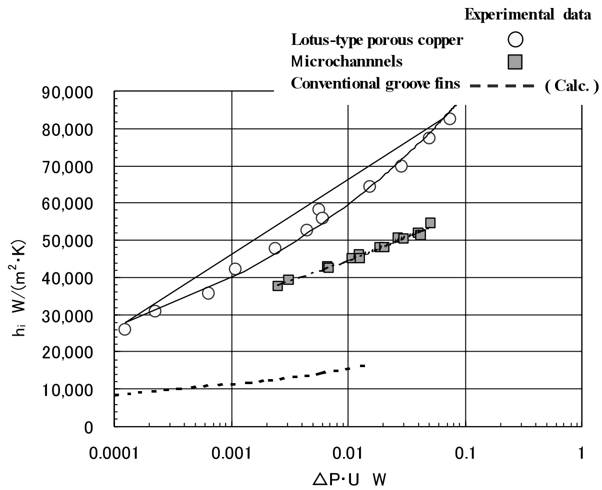

Fig. 11 Comparison of heat transfer h_i as a function of pumping power

groove fins.

The heat-transfer coefficient h_i is shown as a function of pumping power and is defined by the product of flow rate U and ΔP, as shown in Fig. 11. A comparison of the heat transfer coefficients among all of the heat sinks under a pumping power of 0.01 W reveal that the experimental data for the lotus-type copper heat sink is 1.3 times greater than that of the micro-channels and 4 times greater than that of the conventional groove fins.

5. Conclusions

Through on experimental and analytical investigation into the lotus-type porous copper heat sink, we obtained the following conclusions:

(1) Fin efficiency of the lotus-type porous copper fin is verified to be predictable by the straight fin model by using the effective thermal conductivity perpendicular to the pore axis and the surface area ratio between the surface area of the lotus copper and the straight fin.

(2) The heat transfer coefficient, which is based on the base-plate area and the pressure drop of the lotus-type copper heat sink, can be predicted by using the correlation for cylindrical pipes within an accuracy of ±15% and ±5%, respectively.

(3) The heat transfer capacity of the lotus-type porous copper fins was very high and was found to be 4 times greater than the conventional groove fins and 1.3 times greater than micro-channel heat sink under the same pumping power.

References

(1) Weilin, Q., Mala, G.M. and Dongqing, L., Pressure-Driven Water Flows in Trapezoidal Silicon Micro-Channels, Int. J. of Heat and Mass Transfer, Vol.43 (2000), pp.353–364.

(2) Wei, X. and Joshi, Y., Stacked Micro-Channel Heat Sinks for Liquid Cooling of Microelectronic Components, Proceedings of ASME IMECE 2000 Int. Mec. Eng. Congress & Exposition, (2000).

(3) Bastawros, A.F., Evans, A.G. and Stone, H.A., Evaluation of Cellular Metal Heat Transfer Media, Preprint for Publication of Journal of Heat Transfer, March (1999).

(4) Nakajima, H., Lotus-Type Porous Metals — Fabrication, Strength and Application —, J. Soc. Powder Technology, Vol.40 (2003), pp.108–114.

(5) Behrens, E., Thermal Conductivities of Composite Materials, Journal of Composite Materials, Vol.2, No.1 (1968), pp.2–17.

(6) Han, L.S. and Cosner, A.A., Effective Thermal Conductivities of Fibrous Composites, Journal of Heat Transfer, Vol.103 (1981), pp.387–392.

(7) Ogushi, T., Chiba, H., Nakajima, H. and Ikeda, T., Measurement and Analysis of Effective Thermal Conductivities of Lotus-Type Porous Copper, Proceedings of 3rd Int. Conf. on Cellular Metals and Metal Foaming Technology, (2003), pp.1–6.

(8) Shah, R.K. and London, A.L., Laminar Flow Forced Convection in Ducts, Advances in Heat Transfer Suppl., Vol.1 (1978), p.192.

(9) Shah, R.K., A Correlation for Laminar Hydrodynamic Entry Length Solutions for Circular and Noncircular Ducts, J. Fluids Eng., Vol.100 (1978), p.177.

(10) Dittus, F.W. and Boelter, L.M.K., Heat Transfer in Automobile Radiators of the Tubular Type, Univ. Calif. (Berkeley) Pub. Eng., Vol.2 (1930), p.443.